SPOT-VEG BASED ANALYSIS OF SIBERIAN SILKMOTH OUTBREAK

VIATCHESLAV.I. KHARUK[1], K. JON RANSON[2] AND SERGEY T. IM[1]

[1]V. N. Sukachev Institute of Forest, Krasnoyarsk, Russia (kharuk@ksc.krasn.ru).
[2]NASA's Goddard Space Flight Center, Greenbelt, MD 20771, USA
(kenneth.j.ranson@nasa.gov).

The Siberian forests are the habitat of many insect species. Periodic outbreaks of certain insect pests cause a decrease in tree growth, forest decline or mortality over vast areas. The Siberian silkmoth (*Dendrolimus superans sibiricus,* Tschetw) feeds heavily on needles of certain tree species, rapidly defoliating and killing large stands of trees. Outbreaks seem to be influenced by topography. Remote sensing offers a tool for monitoring insect outbreaks over large areas however, not much has been reported in the literature about this. In this paper we looked at the use of data from the French SPOT-Vegetation satellite for insect pest monitoring.

The spatial and temporal dynamics of an outbreak of the Siberian silkmoth were correlated with topographic features of the affected area using SPOT-VEG data and a high resolution digital elevation model (DEM). In 2002-2003 an outbreak affected ~20,000 ha in the South Siberian mountains of Russia. The outbreak began between the elevations of ~430- 480 m and on southwest slopes with steepness < 5°. As the pest searched for food it moved up and down slope, resulting in an elevation distribution split within a range of ~390-540 m and slope steepness up to 15°. In the final phase the azimuth distribution of damaged stands became even. The correlation between the initial phase and topographic features can be used to prioritize monitoring forest areas most vulnerable to destruction by pests.

The significance of satellite-based pest monitoring should increase in the context of climate change. The nutrition base of Siberian silkmoth , so called "dark needle stands" composed by fir and Siberian pine, is within the zone of most intensive observed and predicted climate warming. Nowadays the zone of potential outbreaks is limited to ~59 deg north latitude and by severe climate. Siberian silkmoth is a natural component of

taiga ecosystems at higher latitudes too. As a response to warming, it's expected that outbreaks will occur at higher latitudes, alongside with an increase of outbreak frequency and area of damaged stands in the south. Observed penetration of the Siberian silkmoth host species to the north, into currently larch dominated communities will, in the long term, lead to a vast increase a nutrition base of this pest. Due to the geographic scale and remoteness of taiga landscapes vulnerable to Siberian silkmoth outbreaks, Spot-VEG type sensors should be used in pest monitoring.

SPOT-VEG BASED ANALYSIS OF SIBERIAN SILKMOTH OUTBREAK

VIATCHESLAV.I. KHARUK[1], K. JON RANSON[2] AND SERGEY T. IM[1]

[1]V. N. Sukachev Institute of Forest, Krasnoyarsk, Russia (kharuk@ksc.krasn.ru).
[2]NASA's Goddard Space Flight Center, Greenbelt, MD 20771, USA (kenneth.j.ranson@nasa.gov).

The spatial and temporal dynamics of an outbreak of the Siberian silkmoth were correlated with topographic features of the affected area using SPOT-VEG data and a high resolution digital elevation model (DEM). In 2002-2003 an outbreak affected ~20,000 ha in the South Siberian mountains of Russia. The outbreak began between the elevations of ~430- 480 m and on southwest slopes with steepness < 5°. As the pest searched for food it moved up and down slope, resulting in an elevation distribution split within a range of ~390-540 m and slope steepness up to 15°. In the final phase the azimuth distribution of damaged stands became even. The correlation between the initial phase and topographic features can be used to prioritize monitoring forest areas most vulnerable to destruction by pests.

Key words: Siberian silkmoth outbreaks, SPOTvegetation, monitoring, 3D analysis

INTRODUCTION

The Siberian forests are the habitat of many insect species. Periodic outbreaks of certain insect pests cause a decrease in growth increment, forest decline or mortality over vast areas. The Siberian silkmoth (*Dendrolimus superans sibiricus,* Tschetw) feeds heavily on needles of certain tree species, defoliating and killing large stands rapidly. This is one of the primary factors of taiga succession.

The preferred pest host species are fir (*Abies sibirica*), Siberian pine (*Pinus sibirica*) but spruce (*Picea obovata*) and larch (*Larix sibirica*) are also sometimes affected. Outbreaks are encouraged by favorable weather conditions: low summer precipitation, relatively mild winters with stable, dense snow cover and lack of late spring and early autumn frosts. On the contrary, cold, rainy summers and severe low-snow winters are not favorable for the Siberian silkmoth. Outbreaks have a periodicity, occurring about every 15-25 years. Between 1878 and 2004 ten Siberian silkmoth outbreaks were observed in the Yenisey River watershed area. The largest outbreak (1954-57) resulted in tree damage over about 4 million ha and tree mortality on about 1.5 million ha (Kharuk et al, 2003, 2004). The last outbreak occurred in the south Siberian mountain taiga in 2002-2003 yrs (fig. 1). Outbreaks of insect pests promotes wildfires, because pest-killed stands accumulate combustible material in form of dead wood, grass and bush communities.

Satellite data are an effective tool for detecting, mapping and monitoring of outbreaks (Nelson, 1983; Dottavio and Williams, 1983; Royle and Lathrop, 1997, 2002; Gilli and Gorla, 1997). Spaceborn instruments that provide higher resolution data (e.g., Landsat) are applicable for analysis of forest vigor and large-scale forest damage mapping (Luther et al, 1997; Radeloff et al., 1999; Kharuk et al., 2003). However, there are surprisingly few reports on coarse spatial resolution satellite data application for monitoring insect-induced tree defoliation and mortality (Gilli and Gorla, 1997; Kharuk et al., 2004; Fraser and Latifovic, 2005). The recent Siberian silkmoth outbreak (2002-2003) provides an opportunity to test the latest generation of coarse resolution spectroradiometers (SPOT-VEG, Terra/MODIS) for pest monitoring. Combination of this satellite data with available high-resolution 3D models (USGS, 2007) provides a tool for spatial analysis of outbreak dynamics which can reveal the relationship between outbreak patterns and relief features (elevation, azimuth, slope steepness). This can allow prioritization of monitoring for the detection of the initial phase of an insect outbreak,. Early detection is an important factor for effective pest control and outbreak suppression.

The purpose of this paper is to analyze the spatial and temporal dynamics of a Siberian silkmoth outbreak based on SPOT-VEG data and a digital elevation model (DEM).

Materials and method

The most recent known Siberian silkmoth outbreak began in 2002 in the Eastern Sayan Mountains of Russia., resulting in tree mortality on 16,520 ha, according to on-ground data (Rosleszashita, 2005) (fig. 1). This area has severe continental climate. The mean annual temperature is -1.5 to -6,5 °C. Temperatures in the January, the coldest month, fall to -50°C while temperatures in July, the warmest month, may reach +17 to +19 °C. Mean annual precipitation is about 450-550 mm with the majority (60-70%) falling during summer. Mean relative humidity is 70-75% with maximum values in November-January and minimum in April-June. Stable snow cover lasts over 5 months normally from 1 November till 1 May. The growing season is 115-150 days. The outbreak was located in the vast watershed territory with relatively flat landscape with elevations up to 700 m. The dominant host species in the outbreak area were fir and Siberian pine.
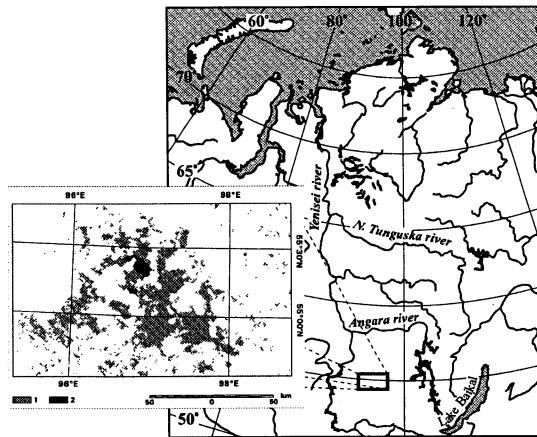
Fig. 1. Siberian silkmoth outbreak location. Insert is SPOT-VEG based classification of outbreak area. 1. non-damaged stands, 2. outbreak area.

Satellite (SPOT-VEG, Landsat) data, a forest inventory map (1: 100,000 dated by 1996 yr), and an insect damage map (of 1:100,000 dated by 2004 yr) were used in the analysis. The insect damage map illustrated two categories: insect-killed and non- damaged stands. Data were processed using Erdas Imagine and Statsoft Statistica software (Erdas Field Guide, 1999; StatSoft, Inc. 2003). The classification accuracy was evaluated by examing the classification confusion matrix and κ-statistics (Erdas Field Guide, 1999).

Image analysis

SPOT-VEG data consisted of ten-day composites (24 scenes total, product S10, HDF format, Platte Carree projection, 16 bits radiometric resolution). The SPOT-VEG data were referenced to the middle of the ten-day compositing interval. Composites contained four spectral bands (430-470, 610-680, 780-790, and 1580-1750 nm) with 1×1 km pixel size.

Ladsat-7 data (6 scenes) were used as an additional information source; this sensor is useful for host species and outbreak area detection (Kharuk et al., 2003). The analyzed scene fragments on the study area were essentially cloud free (< 5% of cloud).

A high resolution DEM based on the US SRTM data was used for outbreak pattern analysis (spatial resolution of 90 m and vertical resolution of ±15 m; USGS 2007). The outbreak area was analyzed with respect to eight slope aspect categories [(1) North (aspect angle range of 338°- 360° and 0°--22°); (2) Northeast (23°--68°), (3) East (69° -- 113°); (4) Southeast (114° -- 158°); (5) South (159° - - 203°); (6) Southwest (204° -- 248°); (7) West (249° -- 293°); (8) Northwest (294° -- 337°)].

The distribution of topographic elements (altitude, azimuth and slope steepness) within the analyzed area is uneven; this could bias the results of the analysis. To make the analysis non-biased,

areas with a given damage category and with given azimuth, slope steepness and elevation were
matched to areas with the similar parameters within the entire damaged area:

$$\kappa_{c(i)} = A_{c(i)-f} / A_{c(i)-I}$$

where the $c_{(i)}$ subscript represents the ith category of landcover feature c, $A_{c(i)-f}$ is the area of
the given on-ground class within the ith category of the topography feature c, and $A_{c(i)-I}$ is the area of
the ith category of topography feature c over the entire analyzed area.

Data analysis included: 1) NDVI dynamics; 2) Damaged stand area dynamics; 3) correlation
analysis of outbreak area dynamics and relief features (elevation, azimuth, slope steepness). Training
sample selection was based on inventory and insect damage maps and Landsat data. The region
growing method was used to form the training sample area. Since training sample statistics were
found to be normally distributed, the maximum likelihood classification and threshold utility method
were applied. Threshold utility allows to select study classes based on classifier distance and adjusting
confidence level α ($\alpha = 0.01-0.3$). Minimal calculated classifier distances for each pixel were used in
analysis.

The analyzed area included only two Siberian silkmoth host species (fir and Siberian pine).
This allowed exclusion of background classes (such as deciduous stands, cuts, shrubs, etc), thus
decreased classification error. For this purpose a "host species" mask was generated based on pre-
outbreak SPOT-VEG scenes.

The temporal set of SPOT-VEG based classification maps were generated that covered the
period from 1999-2004 . Map generation included these steps: 1. Noise reduction by median filtering
(3 x 3 window). 2. "Host species" stand mask application. 3. Removal from analysis previously
damaged stands identified from existing insect damage maps.

Table 1 and 2 represent the training area data and classification accuracy statistics. Note that for the
beginning of the outbreak (Table 2, lines 2-4) the accuracy is poor . This is dues to the difficulty of
classifying insect damage at the earliest stages. As the outbreak develops classification accuracy
becomes satisfactory. (Table 2).

Table 1. Ttraining set data for classification map generation

No	Class/acquisition date	Number of samples	Number of pixels	Mean SPOT-Vegetation channels brightness				Standard deviation			
				1	2	3	4	1	2	3	4

No	Class/acquisition date	Number of samples	Number of pixels	Mean SPOT-Vegetation channels brightness				Standard deviation			
				1	2	3	4	1	2	3	4
1	Healthy stands (08/21/99)	7	2391	5.0	52.7	387.0	228.4	4.1	4.8	19.2	12.4
2	Damaged stands (08/01/02)	1	27	16.3	52.5	323.5	184.7	0.5	0.6	1.3	2.6
3	Damaged stands (08/11/02)	1	24	25.0	40.6	268.4	174.8	1.0	1.0	3.3	3.8
4	Damaged stands (08/21/02)	2	34	361.0	330.9	492.0	292.4	20.2	16.4	14.0	15.2
5	Damaged stands (09/01/02)	4	160	44.2	70.9	244.0	185.1	11.0	5.9	10.8	12.6
6	Damaged stands (09/11/02)	2	254	14.5	52.6	228.7	190.1	10.2	3.6	18.6	12.4
7	Damaged stands (09/21/02)	4	225	64.5	98.9	271.4	233.3	11.0	10.4	19.7	21.1
8	Damaged stands (10/01/02)	2	177	12.5	65.9	179.4	185.8	2.2	3.6	9.0	11.4
9	Damaged stands (10/11/02)	4	323	60.2	107.6	245.8	191.4	12.9	14.2	15.8	12.6
10	Damaged stands (10/21/02)	6	287	53.9	103.9	253.2	203.0	10.8	11.5	16.9	18.1
11	Damaged stands (02/21/03)	5	253	194.7	184.4	291.0	192.4	14.4	15.5	17.1	12.4
12	Damaged stands (08/21/03) acquisition date	2	271	19.7	41.3	217.2	213.1	2.0	3.3	11.3	10.0
13	Damaged stands (08/21/04)	2	322	5.6	47.6	265.9	213.8	1.3	2.5	12.7	9.5

Table 2. Classification accuracy

No	Class	N_f	N_s	N_c	A_c	A_u	E_o	E_e	K_c	K_o

No	Class	N_f	N_s	N_c	A_c	A_u	E_o	E_e	K_c	K_o
1	"Host species " stands mask (08/21/99)	52	34	32	61.54%	94.12%	38.46%	5.88%	0.88	0.57
2	Damaged stands (08/01/02)	39	3	3	7.69%	100.00%	92.31%	0.00%	1.00	0.09
3	Damaged stands (08/11/02)	39	3	3	7.69%	100.00%	92.31%	0.00%	1.00	0.09
4	Damaged stands (08/21/02)	39	4	4	10.26%	100.00%	89.74%	0.00%	1.00	0.12
5	Damaged stands (09/01/02)	39	24	23	58.97%	95.83%	41.03%	4.17%	0.93	0.62
6	Damaged stands (09/11/02)	39	37	36	92.31%	97.30%	7.69%	2.70%	0.96	0.92
7	Damaged stands (09/21/02)	39	37	36	92.31%	97.30%	7.69%	2.70%	0.96	0.92
8	Damaged stands (10/01/02)	39	37	36	92.31%	97.30%	7.69%	2.70%	0.96	0.92
9	Damaged stands (10/11/02)	39	37	36	92.31%	97.30%	7.69%	2.70%	0.96	0.92
10	Damaged stands (10/21/02)	39	37	36	92.31%	97.30%	7.69%	2.70%	0.96	0.92
11	Damaged stands (02/21/03)	39	39	37	94.87%	94.87%	5.13%	5.13%	0.92	0.92
12	Damaged stands (08/21/03)	39	39	37	94.87%	94.87%	5.13%	5.13%	0.92	0.92
13	Damaged stands (08/21/04)	39	39	37	94.87%	94.87%	5.13%	5.13%	0.92	0.92

N_f – number of reference points; N_s – number of classified points; N_c – number of correctly identified reference points; A_c, A_u – classifier and user accuracy; E_o, E_e – omission and commission errors; K_c – current class κ-statistics value; K_o – overall κ-statistics value.

Results

The temporal dynamics of the NDVI and ΔNDVI for pre-outbreak (1999-2001), outbreak (2002), and post-outbreak (2003-2004) periods is shown on fig. 2.
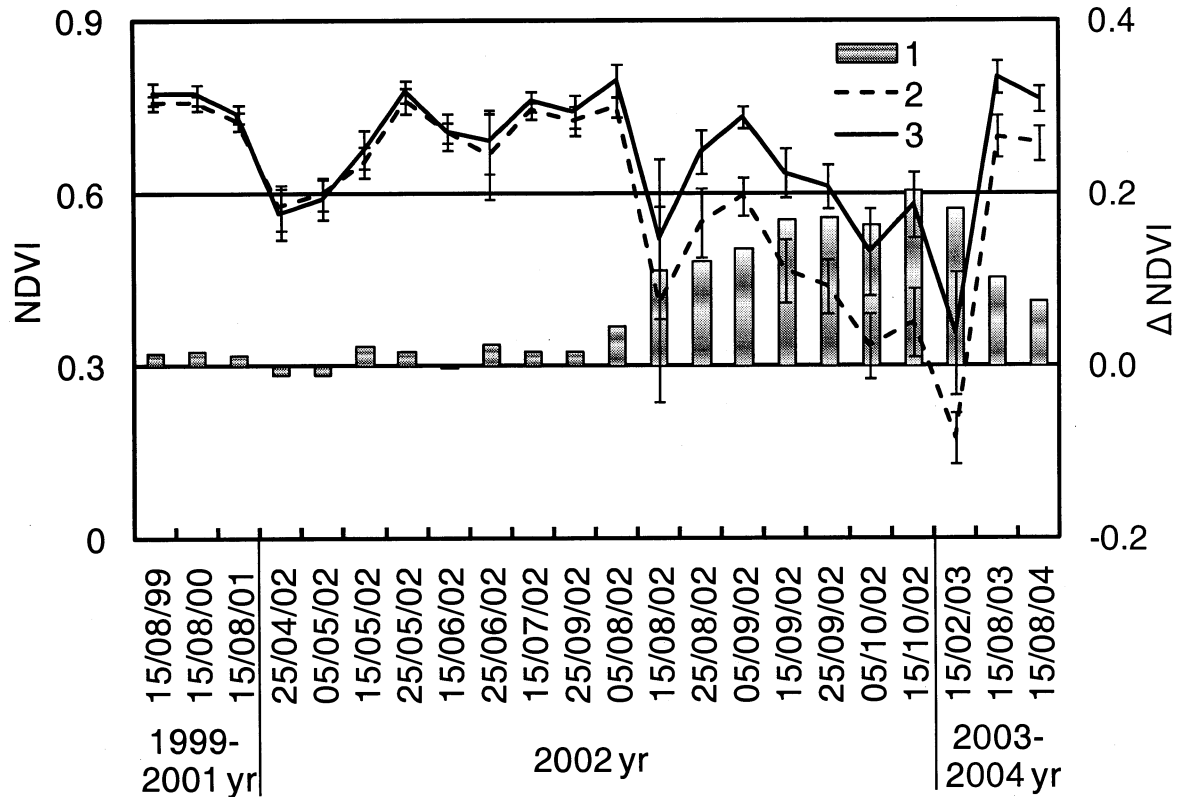
Fig. 2. NDVI dynamics of Siberian silkmoth outbreak and control areas.

1 – ΔNDVI (a difference between control and outbreak stands),
2 –NDVI of damaged stands, 3 – NDVI of control stands.
Bars shows a confidence level (p<0.05).

The NDVI profiles were generated based on temporal data from outbreak and areas of no insect damage (control areas) (Table 1). ΔNDVI is the difference between NDVI values for the control and outbreak areas. In three years prior to the outbreak (1999 - 2001) there were no significant NDVI difference between the outbreak and control areas. Therefore, on the time axis in Table 1 each year is represented by a single mid-August data point The ΔNDVI difference becomes significant starting end of July 2002 (fig. 2) when the insect outbreak began. In both the outbreak and control areas NDVI decreases in the mid August (08/15/2002) with a larger NDVI decrease in the outbreak area. This decrease is attributed to decrease in SPOT-VEG composite quality caused by haze on the ground. Starting mid-September the ΔNDVI differences stabilized. The NDVI decline observed at the end of September was caused by phenology changes. Note that ΔNDVI for the winter-acquired image (02/15/2003) is also high. During the following years' growing seasons (2003 – 2004) the ΔNDVI decreased.
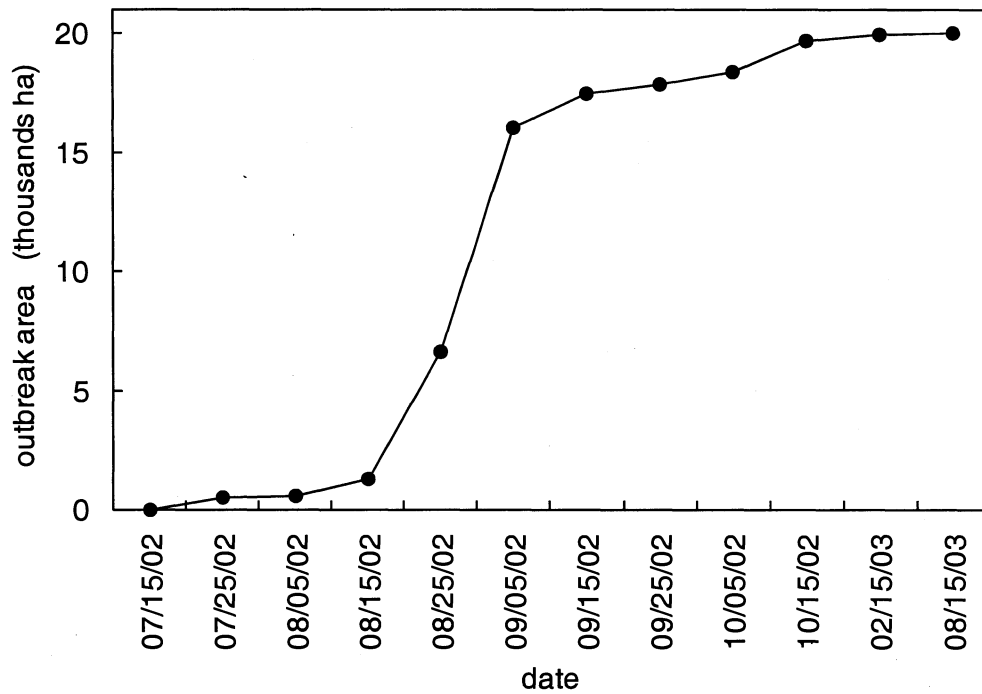
Fig. 3. Insect outbreak area over time

The outbreak area plotted over time forms a logistic type curve with a lag-phase following by a rapid increase of defoliated area during next two years after which it levels off (Fig. 3).

The elevation of the initial outbreak phase ranged from ~430 to 480 m as the outbreak continued, the elevation range expanded from ~390 to 540 m. (Fig. 4) During this period the area of the outbreak increment (the difference in outbreak area in relative units) the distribution becomes bi-modal.
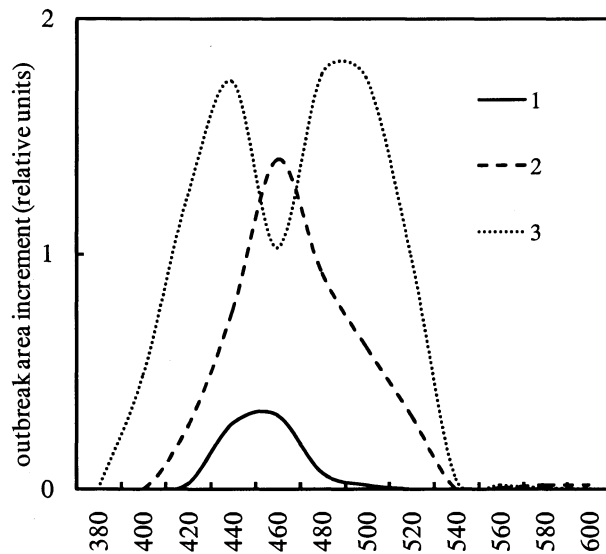
Fig. 4. Change in outbreak area increment with respect to elevation.

1, 2, 3 – increment of outbreak areas for the period of 08/11/02-08/21/02,
08/21/02-09/01/02 and 09/01/02-09/11/02, correspondingly.
The area increment was calculated as outbreak area distribution for given the dates.

The insect outbreak began on gentle slopes of $< 5°$. As the outbreak expanded, areas with slope steepness up to 15° became affected (Fig. 5). The slope aspect of the outbreak area also changed over time. Initial damage was found on slopes with a southwestern aspect. Later, damage occurred more frequently on slopes with a western aspect. By the end of the outbreak, the slope aspect became more evenly distributed. (Fig. 6).
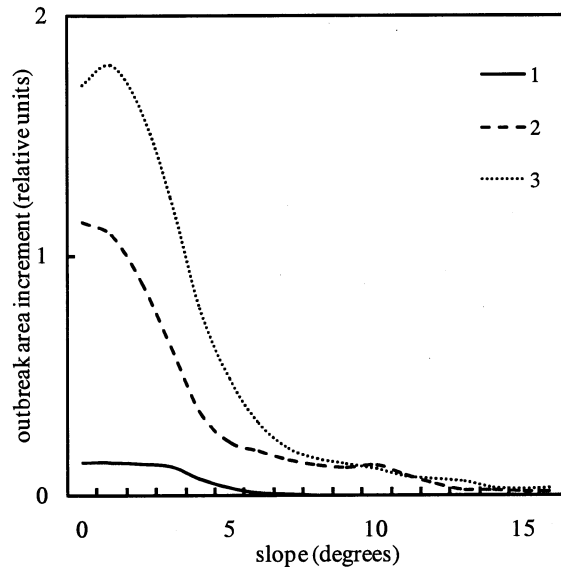

Fig. 5. Outbreak area increment dynamics with respect to slope steepness.

1, 2, 3 – increment of outbreak areas for the period of 08/11/02-08/21/02,
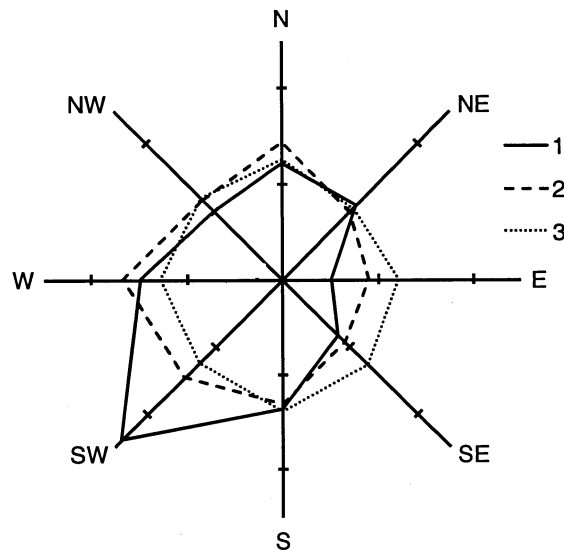08/21/02-09/01/02 and 09/01/02-09/11/02, respectively.

Fig. 6. Outbreak area dynamics with respect to slope aspect.

Outbreak area 1 – 08/11/02, 2 – 09/01/02, 3 – 21/08/03

Discussion

In the area of study, a population increase of the Siberian silkmoth caterpillar was observed in 1998 (Rosleszashita, 2005). However, it was not until 2002 that an outbreak of the insect pest occurred. Using SPOT-VEG data the first indication of Siberian silkmoth outbreak was detected at the end of July 2002, when the difference between NDVI of healthy and damaged stands became significant (Fig. 2). During the next three years of the active outbreak about ~17 000 ha of forests were completely defoliated. A further increase in the outbreak area was due to mortality of weakened trees and, presumably secondary pest damage such as caused by the bark beetle (*Monochamus urussovi*, Fish). In the years following the outbreak (2003, 2004) NDVI differences between outbreak and control areas decreased due to growth of grass, shrubs, and deciduous trees. .

Because snow cover reduces the influence of the background the NDVI difference between healthy and damaged stands is also high during the winter. This indicates that winter acquired images are potentially useful in pest monitoring. *NB: check and make sure this references a point in the prior text*

In previous insect outbreaks affecting the Sayan mountain region, the maximum insect induced stand defoliation is typically observed during late June through the beginning of July. The defoliation in this outbreak peaked later, *during September vis a vis Figure 3 NB:check fact*. This time-shift could be attributed to two factors. First, the defoliation may have been caused by presence of more than one silkmoth generations (with one- and two-years life cycles) rather than one generation. Second, this outbreak occurred at relatively high elevations (390 – 520 m) compared to the majority of reported

outbreaks in the area which have been located in lowlands. Thus the impact of the local climate could be a factor in the timing of the peak of maximum defoliation.

Earlier researchers empirically observed that the outbreaks begin in the best pest habitat sites (Isaev and Kondakov, 1986). The satellite data obtained shows that the spatial development of the outbreak was also related to topographic features. Because the initial outbreak phase occurred on gentle (<5°) southwest slopes within the elevation range of 420-500 m, these conditions appear to be the most favorable pest habitat (Fig. 4, 5). As food resources were depleted the pest migrated to less suitable areas with slopes up to 15° (Fig.5) and to both higher and lower elevations, expanding the elevation range to 390-540 m. This created a bi-modal distribution of elevation shown in Figure 4.

In order to minimize forest damage, it is crucial to detect the initial stages of Siberian silkmoth outbreaks. The combined satellite-derived NDVI and DEM analysis revealed the topographic characteristics of sites where the outbreak began. This knowledge is essential for prioritizing areas to monitor for the first signs of silkmoth outbreak damage. It's necessary to emphasize that the spatial pattern data are not biased, i.e. the normalization used provides results which are independent of the absolute areas with given topographic features. Moreover, data were normalized with respect to the area covered with host species. Otherwise the final result has to be dependant on the initial host species distribution: if this distribution is non- even with respect to topography, the resulting spatial outbreak pattern will be biased.

The final SPOT-VEG derived outbreak area was about 20,000 ha, which is about 12% higher than the area reported by data collected in the field (Rosleszashita, 2005). This difference actually is within field collected data measurement error, which is about10-15%. The outbreak area in this study is relatively small. The outbreak size was limited by weather conditions unfavorable for the insect pest species and, partially by suppression measures. In comparison, during a previous outbreak (1993-1995) that occured between the Yenisey and Angara rivers, the Siberian silkmoth affected stands on ~700,000 ha and caused tree mortality on about 300,000 ha. This scale of damage allows applying NOAA/AVHRR data for outbreak analysis (Kharuk et al, 2004). The data analyzed here shows that even small-size outbreaks could be analyzed based on SPOT-VEG images: the outbreak area of about 4 pixels in size (400 ha) was detectable (fig. 2, 3). Nevertheless, application of higher resolution data (e.g., Landsat, SPOT) is necessary for early detection of initial outbreak phases, which is important for effective pest control. Unfortunately high resolution data are non available with the needed frequency. There also are temporal "gaps" between data acquisition for the same area. For Landsat it is 16 days, the period comparable with active phase of outbreak dynamics (fig. 3). On the contrary, SPOT-VEG and Terra/MODIS data are available at the daily scale.

An important problem is the indication of the intermediate levels of stand defoliation. In our study we were limited by maps derived from on-ground data with only two classes: healthy and

completely defoliated stands. Thus, only the dynamics of silkmoth-killed stands were analyzed. Whereas SPOT-VEG sensor should be sensitive to the less defoliated stand categories; this conclusion is based on the study of AVHRR application: also this sensor is less sensitive thans SPOT-VEG, three stand categories were detected (healthy, completely and intermediately defoliated; Kharuk et al, 2004). For the further progress it's necessary to combine timely organized on-ground studies with satellite-based observations during next Siberian silkmoth outbreak.

Finally, the significance of satellite-based pest monitoring should increase in the context of climate change. The nutrition base of Siberian silkmoth , so called "dark needle stands" composed by fir and Siberian pine, is within the zone of most intensive observed and predicted climate warming (Zwiers, 2002). Nowadays the zone of potential outbreaks is limited to ~59 deg north latitude and by severe climate. Siberian silkmoth is a natural component of taiga ecosystems at higher latitudes too. As a response to warming, it's expected that outbreaks will occur at higher latitudes, alongside with an increase of outbreak frequency and area of damaged stands in the south. Observed penetration of the Siberian silkmoth host species to the north, into currently larch dominated communities (Kharuk et al., 2005) will, in the long term, lead to a vast increase a nutrition base of this pest. Due to the geographic scale and remoteness of taiga landscapes vulnerable to Siberian silkmoth outbreaks, SpotVeg type sensors should be used in pest monitoring.

Acknowledgment

References

Dottavio, C. L. and Williams, D. L., 1983, Satellite technology- an improved means for monitoring forest insect defoliation. *J. Forestry,* 81(1), 30-34.

Erdas Inc. 1999. *Erdas Field Guide* (5th ed. Revised and Expanded. Atlanta, Geogia: Erdas Inc.).

Fraser, R.H. and Latifovic, R., 2005, Mapping insect-induced tree defoliation and mortality using coarse spatial resolution satellite imagery. *International Journal of Remote Sensing*, 26(1), 193-200.

Gilli, M. P. and Gorla, D. E., 1997, The spatio-temporal pattern of Delphacodes kuscheli (Homoptera: Delphacidae) abundance in central Argentina. *Bull. Entom. Resear*, 87(1), 45-53.

Isaev, A. S. and Kondakov, Y. P., 1986, The principles and methods of forest-entomological monitoring. *Lesovedenie (Russian Forest Journal)*, 4, 3-9 (in Russian).

Kharuk, V. I., Dvinskaya, M. L., Ranson, K. J. and Im, S. T., 2005, Expansion of evergreen conifers to the larch-dominated zone and climatic trends. Russian Journal of Ecology, 36 (3), 164–170.

Kharuk, V. I., Ranson, K. J., Kozuhovskaya, A. G., Kondakov, Y. P., and Pestunov, I. A., 2004, NOAA-AVHRR Satellite Detection of Siberian Silkmoth Outbreaks in Eastern Siberia. *Int. J. Remote Sensing*, 20(24), 5543-5555.

Kharuk, V. I., Ranson, K. J., Kuz'michev, V. V., Im, S. T., 2003, Landsat-based analysis of insect outbreaks in southern Siberia. *Canadian J. Remote Sensing*. 29(2), 286-297.

Luther, J.E., Franklin, S., Hudak, J. and Meades, J.P., 1997, Forecasting the susceptibility and vulnerability of balsam fir stands to insect defoliation with Landsat Thematic Mapper data. *Remote Sensing of Environment*, 59, 77–91.

Nelson, R. F., 1983, Detecting forest canopy change due to insect activity using Landsat MSS. *Photogrammetric Engineering and Remote Sensing*. 1983, 49, 1303-1314.

Radeloff, V. C., Mladenoff, D. J. and Boyce M. S., 1999, Detecting Jack Pine budworm defoliation using spectral mixture analysis: Separating effects from determinants. *Remote Sensing of Environment*, 69(2), 156-169.

Rosleszashita, 2005, *Report on forest health status in the Krasnoyarsk krai regions* (Rosleszashita, Pushkino).

Royle, D. and Lathrop, R., 2002, Discriminating Tsuga canadensis hemlock forest defoliation using remotely sensed change detection. *Journal of Nematology*, 34, 213-221.

Royle, D. D. and Lathrop, R. G., 1997, Monitoring hemlock forest health in New Jersey using Landsat TM data and change detection techniques. *Forest Science*, 43, 327–335.

StatSoft, Inc. 2003, Nonparametric Statistics. Available online at: http://www.statsoft.com/textbook/STNonpar.html.

USGS, 2007, Digital elevation models. Available online at: http://srtm.usgs.gov .

Zwiers F.W. (2002).The 20-year forecast. *Nature*, *416*, 690–691.